Article

On the Electronic Structure and Chemical Bonding in the Tantalum Trimer Cluster

Bin Wang, Hua-Jin Zhai, Xin Huang, and Lai-Sheng Wang

J. Phys. Chem. A, **2008**, 112 (43), 10962-10967 • DOI: 10.1021/jp806166h • Publication Date (Web): 03 October 2008

On the Electronic Structure and Chemical Bonding in the Tantalum Trimer Cluster

Bin Wang,[†,||] Hua-Jin Zhai,[‡,§] Xin Huang,*[,†,||] and Lai-Sheng Wang*[,‡,§]

Department of Chemistry, Fuzhou University, Fuzhou, Fujian 350108, P. R. China, State Key Laboratory of Structural Chemistry, Fuzhou, Fujian 350002, P. R. China, Department of Physics, Washington State University, 2710 University Drive, Richland, Washington 99354, and Chemical & Materials Sciences Division, Pacific Northwest National Laboratory, MS K8-88, Post Office Box 999, Richland, Washington 99352

Received: July 12, 2008; Revised Manuscript Received: August 27, 2008

The electronic structure and chemical bonding in the Ta_3^- cluster are investigated using photoelectron spectroscopy and density functional theory calculations. Photoelectron spectra are obtained for Ta_3^- at four photon energies: 532, 355, 266, and 193 nm. While congested spectra are observed at high electron binding energies, several low-lying electronic transitions are well resolved and compared with the theoretical calculations. The electron affinity of Ta_3 is determined to be 1.35 ± 0.03 eV. Extensive density functional calculations are performed at the B3LYP/Stuttgart +2f1g level to locate the ground-state and low-lying isomers for Ta_3 and Ta_3^-. The ground-state for the Ta_3^- anion is shown to be a quintet ($^5A_1'$) with D_{3h} symmetry, whereas two nearly isoenergetic states, C_{2v} ($^4A_1$) and D_{3h} ($^6A_1'$), are found to compete for the ground-state for neutral Ta_3. A detailed molecular orbital analysis is performed to elucidate the chemical boding in Ta_3^-, which is found to possess multiple d-orbital aromaticity, commensurate with its highly symmetric D_{3h} structure.

1. Introduction

Transition metals exhibit diverse physical and chemical properties and offer unique opportunities in advancing chemical bonding models. The milestone work of Cotton and co-workers[1] on δ-bond in the $Re_2Cl_8^{2-}$ compound[2] has led to the development of a new branch of inorganic chemistry on multiple metal−metal bonding.[3−7] The recent synthesis of a Cr_2 compound with a quintuple bond ($\sigma^2\pi^4\delta^4$)[4] has generated renewed interest in multiple metal−metal bonding.[6−8] In particular, Roos and co-workers[6] have presented computational evidence that the W_2 dimer reaches a bond order of six, the highest possible between any two atoms in the Periodic Table. Delocalized multicenter bonding in transition metal systems also raises the interesting possibility for d-orbital aromaticity and, in particular, δ-aromaticity, which has been actively pursued lately.[9−15] The first examples of d-orbital aromaticity (albeit with σ character) appear to be the $W_3O_9^{2-}$ and $Mo_3O_9^{2-}$ clusters.[12] Very recently, experimental and theoretical evidence has been reported for the first δ-aromatic molecule in $Ta_3O_3^-$.[13] New computational evidence has been presented[15] about triple (σ-, π-, and δ-) aromaticity in the lowest D_{3h} ($^1A_1'$) singlet state of Hf_3. δ-Aromaticity, which is only possible in transition metal systems, represents a new mode of chemical bonding and may play an important role in multinuclear transition metal compounds.

In the present work, we carry out a combined photoelectron spectroscopy (PES) and density functional theory (DFT) study on the electronic and structural properties in the tantalum trimer cluster and its anion. This work represents a continuation of our research interest in exploring chemical bonding and aromaticity in novel inorganic clusters, all-metal main-group clusters, and transition-metal clusters.[9,11−13,16−19] There have been relatively few previous experimental[20−23] or theoretical[22−25] studies on Ta_3 and Ta_3^-, and our understanding on their structure and bonding is still limited. The ionization potential of Ta_3 was reported in two independent experiments to be 5.58 ± 0.05 eV (ref 20) and 5.60 eV (ref 23). A resonant Raman spectrum was obtained for Ta_3, yielding a symmetric Ta−Ta stretching frequency of 251.7 cm^{-1}.[21] Computationally, there is a recent DFT study on $Ta_3^{+/0/-}$ at the B3LYP/LANL2DZ level,[25] reporting a D_{3h} ($^5A_1'$) ground-state for Ta_3^- and three close-lying states for the Ta_3 neutral cluster, D_{3h} ($^6A_1'$), C_{2v} ($^4A_2$), and C_{2v} ($^4B_2$). An earlier B3P86/LANL2DZ study[23] suggested a C_{2v} structure with three unpaired spins as the lowest energy state, though the electronic state was not specified.

In the current work, we combine PES with DFT calculations to elucidate the electronic structure and chemical bonding for the Ta_3^- cluster. Well-resolved low-lying electronic transitions are used to verify the theoretical calculations. We find that Ta_3^- possesses a quintet ground state ($^5A_1'$) with D_{3h} symmetry. Two nearly isoenergetic states, C_{2v} ($^4A_1$) and D_{3h} ($^6A_1'$), are found to compete for the ground-state for the neutral Ta_3 cluster. A detailed molecular orbital (MO) analysis reveals that the Ta_3^- (D_{3h}, $^5A_1'$) cluster possesses multiple (δ, and partial π and σ) aromaticity, which is responsible for its highly symmetric D_{3h} structure.

2. Experimental and Theoretical Methods

2.1. Photoelectron Spectroscopy. The experiment was carried out using a magnetic-bottle PES apparatus equipped with a laser vaporization supersonic cluster source. Details of the apparatus have been described elsewhere.[26] Briefly, the Ta_n^- clusters were produced by laser vaporization of a pure tantalum disk target in the presence of a He carrier gas and analyzed using a time-of-flight mass spectrometer. The Ta_3^- cluster of current interest was mass-selected and decelerated before being photodetached. Four detachment photon energies were used in the experiment: 532 (2.331), 355 (3.496), 266 (4.661), and 193 nm (6.424 eV). Effort was made to choose colder clusters for

* To whom correspondence should be addressed. E-mail: xhuang@fzu.edu.cn; ls.wang@pnl.gov.
† Fuzhou University.
|| State Key Laboratory of Structural Chemistry.
‡ Washington State University.
§ Pacific Northwest National Laboratory.

10.1021/jp806166h CCC: $40.75
Published on Web 10/03/2008

photodetachment, which has proved essential for obtaining high quality PES data.[27] Photoelectrons were collected at nearly 100% efficiency by the magnetic-bottle and analyzed in a 3.5 m long electron flight tube. PES spectra were calibrated using the known spectra of Au^- and Cu^-, and the energy resolution of the PES apparatus was $\Delta E_k/E_k \approx 2.5\%$, that is, ~25 meV for 1 eV electrons.

2.2. Density Functional Calculations. The theoretical calculations were performed at the DFT level using the B3LYP hybrid functional.[28−30] A number of structural candidates including different spin states and initial structures were evaluated, and the search for the global minima was performed using analytical gradients with the Stuttgart 14-valence-electron pseudopotentials and the valence basis sets[31,32] augmented with two *f*-type and one *g*-type polarization functions [$\zeta(f) = 0.210$, 0.697; $\zeta(g) = 0.472$] for tantalum as recommended by Martin and Sundermann.[33] Scalar relativistic effects, that is, the mass velocity and Darwin effects, were taken into account via the quasi-relativistic pseudopotentials. Only a selected set of optimized structures (the ground-state and a few low-lying isomers relevant in the discussion of the experimental data) are reported. Vibrational frequency calculations were performed at the same level of theory to verify the nature of the stationary points.

The B3LYP geometries of selected isomers were tested in single-point energy calculations with other functionals (see Supporting Information, Table S1). We employed functionals with and without components of Hartree−Fock exchange to benchmark them for use in predicting the most stable species. BLYP and B3LYP functionals show similar behavior. The three functionals give the same lowest energy state. As discussed below, B3LYP gives superior results in terms of electron detachment energies when directly compared to experimental results. Therefore, we used the results with B3LYP functional for our further discussion.

Vertical electron detachment energies (VDEs) were calculated using the generalized Koopman's theorem by adding a correction term to the eigenvalues of the anion.[34] The correction term was estimated by $\delta E = E_1 - E_2 - \varepsilon_{HOMO}$, where E_1 and E_2 are the total energies of the anion and neutral, respectively, in their ground states at the anion equilibrium geometry and ε_{HOMO} corresponds to the eigenvalue of the highest occupied molecular orbital (HOMO) of the anion. All the calculations were performed with the Gaussian 03 software package.[35] Three-dimensional contours of the calculated orbitals were visualized using the VMD software.[36]

3. Experimental Results

The PES spectra of Ta_3^- at four photon energies are shown in Figure 1. The low photon energies yield better-resolved spectra for low-lying transitions, whereas the higher photon energies reveal transitions with high electron binding energies. The 532 nm spectrum (Figure 1a) shows three close-lying transitions (X, A, and B). The ground-state VDE was determined from the well-resolved peak maximum of band X as 1.40 ± 0.02 eV (Table 1). Since no vibrational fine structure was resolved, the ground-state adiabatic detachment energy (ADE) was determined by drawing a straight line along the leading edge of band X and then adding the instrumental resolution to the intersection with the binding energy axis. The X band was quite sharp, allowing a fairly accurate ADE to be determined as 1.35 ± 0.03 eV (Table 1), which also represents the electron affinity of Ta_3. Band A at a VDE of 1.52 eV is also very sharp similar to band X. It should represent the first excited-state of Ta_3 because its separation with band X is too large to be due to a vibrational excitation. Band B (VDE: 1.70 eV), which should represent the second excited-state of Ta_3, appears broader

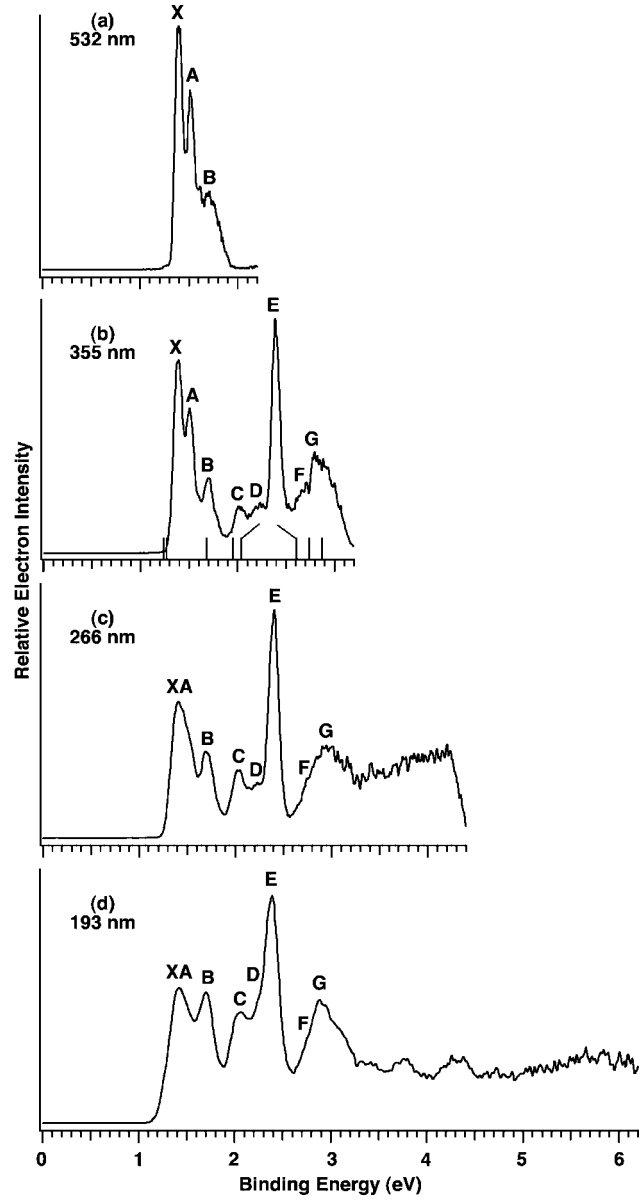

Figure 1. Photoelectron spectra of Ta_3^- at (a) 532 (2.331), (b) 355 (3.496), (c) 266 (4.661), and (d) 193 nm (6.424 eV). Vertical bars in panel b represent the calculated vertical detachment energies from the lowest energy structure of Ta_3^- (D_{3h}, $^5A_1'$).

TABLE 1: Experimental Vertical Detachment Energies (VDEs) of Ta_3^- and Comparison with the Calculated VDEs from the Lowest-Energy Ta_3^- (D_{3h}, $^5A_1'$) Anion[a]

	VDE (exptl)[b]	detachment channel[c]	VDE (theor)
X	1.40(2)[d]	$3a_1'(\beta)$	1.24[e]
A	1.52(2)	$2e'(\alpha)$	1.27
B	1.70(3)	$3a_1'(\alpha)$	1.68
C	2.03(3)	$1e''(\alpha)$	1.95
D	~2.2	$1e'(\beta)$	2.04
E	2.39(2)	$1a_2''(\beta)$	2.61
F	~2.7	$2a_1'(\beta)$	2.74
G	~2.9	$1e'(\alpha)$	2.87

[a] All energies are in eV. [b] Numbers in the parentheses represent experimental uncertainty in the last digit. [c] Labels "α" and "β" denote majority and minority spins, respectively. [d] Electron affinity of Ta_3: 1.35 ± 0.03 eV. [e] Theoretical ADE: 1.21 eV.

TABLE 2: Calculated Geometric Parameters of Ta_3^- and Ta_3 in Various Electronic States and Their Relative Energies (ΔE) at the DFT/B3LYP Level of Theory[a]

state	symmetry	a (Å)	b (Å)	c (Å)	α (deg)	β (deg)	ΔE (eV)
				Ta_3^-			
$^1A_1$	C_{2v}	2.334	2.334	2.767	72.7		0.43
$^1A_1'$	D_{3h}	2.423	2.423	2.423	60.0		0.75
$^3A''$	C_s	2.499	2.323	2.602	65.2	54.1	0.17
$^3A_1$	C_{2v}	2.504	2.504	2.431	58.1		0.32
$^3A_2$	C_{2v}	2.573	2.573	2.281	52.6		0.18
$^3B_1$	C_{2v}	2.503	2.503	2.403	57.4		0.29
$^3B_2$	C_{2v}	2.559	2.559	2.348	54.6		0.54
$^5A_1'$	D_{3h}	2.466	2.466	2.466	60.0		0.00
$^5A_2$	C_{2v}	2.449	2.449	2.568	63.2		0.12
$^5A_1$	C_{2v}	2.428	2.428	2.777	69.8		1.12
$^7B_2$	C_{2v}	2.502	2.502	2.623	63.2		0.64
$^7A_2''$	D_{3h}	2.498	2.498	2.498	60.0		0.76
				Ta_3			
$^2B_1$	C_{2v}	2.424	2.424	2.500	62.1		0.20
$^2A_2$	C_{2v}	2.465	2.465	2.360	57.2		0.28
$^2B_2$	C_{2v}	2.343	2.343	3.202	86.2		1.68
$^2A_1$	C_{2v}	2.373	2.373	2.809	72.6		0.66
$^2B_2$	C_{2v}	2.444	2.444	2.548	62.9		0.76
$^2A_1'$	D_{3h}	2.439	2.439	2.439	60.0		0.38
$^4A_2$	C_{2v}	2.413	2.413	2.607	65.4		0.11
$^4B_2$	C_{2v}	2.341	2.341	3.188	85.8		1.41
$^4B_1$	C_{2v}	2.474	2.474	2.477	60.1		0.40
$^4A_1$	C_{2v}	2.448	2.448	2.537	62.4		0.00
$^4B_2$	C_{2v}	2.431	2.431	2.653	66.1		0.57
$^6A_1'$	D_{3h}	2.506	2.506	2.506	60.0		0.02
$^8B_2$	C_{2v}	2.466	2.466	2.782	68.7		1.31

[a] Structure parameters (a, b, c, α and β) are defined in Figure 2.

(Figure 1a), indicating a large geometry change in this detachment channel between the anion and the neutral final state.

At 355 nm (Figure 1b), a number of higher binding energy features are observed, which appear rather congested. Two relatively weak bands are observed with VDEs of 2.03 eV for band C and ~2.2 eV for band D. A sharp and intense band E is observed at a VDE of 2.39 eV. Beyond 2.5 eV, two broad bands can be tentatively identified at VDEs of ~2.7 eV for band F and ~2.9 eV for band G. The 266 nm (Figure 1c) and 193 nm (Figure 1d) spectra display continuous signals beyond ~2.5 eV and do not yield well-resolved features. The congested spectral features at higher binding energies suggest a very high density of electronic states, which is not surprising for an expected open-shell cluster. Multielectron transitions are also possible, contributing to the spectral congestions at higher binding energies.

4. Theoretical Results

The trimer is a relatively small cluster and there can be only four possible atomic arrangements: linear, equilateral triangle (D_{3h}), isosceles triangle (C_{2v}), or completely distorted triangle (C_s). In our theoretical calculations, we considered all these initial geometries and different spin multiplicities. A selected set of optimized low-lying structures and electronic states for Ta_3^- and Ta_3 are summarized in Table 2 (organized according to the spin multiplicity), along with their equilibrium geometries and relative energies. The geometrical parameters for the triangles are defined in Figure 2.

4.1. Ta_3^-. The ground-state of Ta_3^- is found to be a quintet state $^5A_1'$ with D_{3h} symmetry and a Ta−Ta bond length of 2.466 Å (Table 2). An isosceles triangle C_{2v} ($^5A_2$) also with a quintet state is found to be only 0.12 eV higher. We further located two low-lying triplet states C_s ($^3A''$) and C_{2v} ($^3A_2$) for Ta_3^-, 0.17 and 0.18 eV above the ground state, respectively. The lowest singlet state (C_{2v}, $^1A_1$) is found to be 0.43 eV above the ground state, whereas the lowest heptet state (C_{2v}, $^7B_2$) is 0.64 eV above the ground state. Our theoretical results clearly show that the Ta_3^- anion has a propensity to adopt a quintet D_{3h} ($^5A_1'$) ground state, in agreement with a previous theoretical study[25] at the B3LYP/LANL2DZ level of theory. The high spin ground-state for Ta_3^- is quite remarkable. For comparison, available literature suggests that the isovalent V_3^- (ref 37) and Nb_3^- (ref 38) clusters possess triplet ground states.

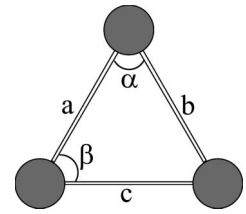

Figure 2. Definitions of structural parameters for Ta_3^- and Ta_3 used in Table 2 for the different isomers.

4.2. Ta_3. Some 13 optimized electronic states for Ta_3, ranging from low-spin doublets to a high-spin octet, are also presented in Table 2. A quartet state ($^4A_1$) with C_{2v} symmetry is found to be the global minimum. However, a sextet state ($^6A_1'$) with D_{3h} symmetry is only 0.02 eV higher in energy, competing for the global minimum for Ta_3. Another low-lying quartet state, C_{2v} ($^4A_2$) is only 0.11 eV above the ground quartet state ($^4A_1$). All other quartet states identified are significantly higher in energy, as well as the doublet and octet states. We note that the linear structure $D_{\infty h}$ ($^6\Delta_u$) (Ta−Ta bond length: 2.340 Å) is significantly higher in energy (2.65 eV). The linear anion is also much higher in energy and they are not listed in Table 2. In summary, the C_{2v} ($^4A_1$) (0.00 eV) and D_{3h} ($^6A_1'$) (0.02 eV) states are virtually isoenergetic and should be considered as competitive candidates for the global minimum for the Ta_3 neutral.

The current structures and energetics (Table 2) on Ta_3 agree in general with those from a previous DFT study at the B3LYP/LANL2DZ level of theory,[25] except that the previous study apparently missed the C_{2v} ($^4A_1$) state identified here as the lowest in energy. It is interesting to note that the unspecified lowest energy C_{2v} structure reported by another previous DFT study[23] at the B3P86/LANL2DZ level (a = 2.403 Å, c = 2.589 Å, α = 65.2°) is similar to the C_{2v} ($^4A_2$) state, which is 0.11 eV above the lowest energy C_{2v} ($^4A_1$) state in the current work (Table 2).

5. Discussion

5.1. Comparison between Experiment and Theory. Transition-metal compounds can be very difficult to handle computationally because of the presence of low-lying electronic states and substantial electron correlation effects. Density functional theory is often the method of choice because it can provide a good treatment of the electronic properties of many transition metal clusters.[39] There have been a number of gas-phase experimental and DFT studies on transition metal systems.[40] Those studies have shown that accurate electron detachment energies can be obtained with DFT methods. In the current work, vertical detachment energies were calculated using the B3LYP level.

Because of the open d-shell of Ta ($5d^36s^2$), even the electronic structure for the relatively simple three-atom system poses considerable computational challenges. Both the current and previous theoretical results suggest that the quintet state D_{3h} ($^5A_1'$) is the global minimum for Ta_3^- with a valent electron configuration of $(1a_1')^2(2a_1')^2(1a_2'')^2(1e')^4$

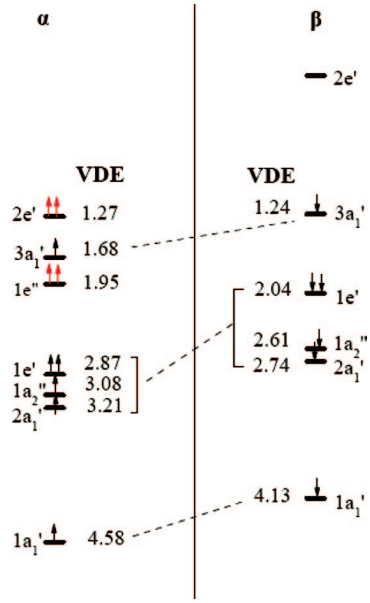

Figure 3. The calculated detachment channels from the Ta_3^- (D_{3h}, $^5A_1'$) ground-state using the generalized Koopman's theorem (see text). The computed vertical detachment energies (VDE) are in eV. The four unpaired spins (in red) in the half-filled 2e′ and 1e″ orbitals lead to the quintet D_{3h} ($^5A_1'$) anion ground state. Comparison with experiment is done in Table 1 and Figure 1b.

$(1e'')^2(3a_1')^2(2e')^2$. The calculated VDEs from these valent MOs are shown in Figure 3 schematically and are used to compare with the experimental data in Table 1. We also calculated the first VDEs of the two close-lying isomers, C_{2v} ($^5A_2$) and C_s ($^3A''$), which are 0.12 and 0.17 eV above the D_{3h} ($^5A_1'$) ground state, respectively (Table 2). The calculated first VDEs are 1.07 eV for the C_{2v} ($^5A_2$) structure and 1.16 eV for the C_s ($^3A''$) structure, compared to the calculated first VDE of 1.24 eV for the D_{3h} ($^5A_1'$) ground state, which is clearly in better agreement with the experimental value of 1.40 eV.

The first detachment channel for the Ta_3^- D_{3h} ($^5A_1'$) ground-state comes from the removal of a $3a_1'(\beta)$ electron (Figure 3), resulting in the lowest sextet neutral state D_{3h} ($^6A_1'$) with five unpaired spins. The sextet state retains the D_{3h} symmetry with a slight increase (0.04 Å) of the Ta−Ta bond lengths (Table 2), consistent with the bonding nature of the $3a_1'$ orbital, as shown in Figure 4. The calculated ADE (1.21 eV) for the first detachment channel or the electron affinity for Ta_3, is also in good agreement with the experimental measurement (1.35 eV). The second detachment channel is from the half-filled $2e'(\alpha)$ MO (Figure 3), leading to the lowest quartet state C_{2v} ($^4A_1$) with three unpaired spins. The computed VDE (1.27 eV) appears to be underestimated by 0.25 eV, compared to the experimental VDE of band A (1.52 eV). The reduced symmetry upon electron detachment from the 2e′ MO is expected, due to the Jahn−Teller effect. However, the A band (Figure 1a) is still quite sharp, consistent with the relatively small geometry change between the C_{2v} ($^4A_1$) neutral state and the ground-state of Ta_3^- (Table 2).

The third and fourth detachment channels are from $3a_1'(\alpha)$ and $1e''(\alpha)$ with calculated VDEs of 1.68 and 1.95 eV (Figure 3), which are in excellent agreement with the experimental VDEs of bands B (VDE: 1.70 eV) and C (VDE: 2.03 eV), respectively. The next predicted detachment channel is from $1e'(\beta)$ with a calculated VDE of 2.04 eV, in good agreement

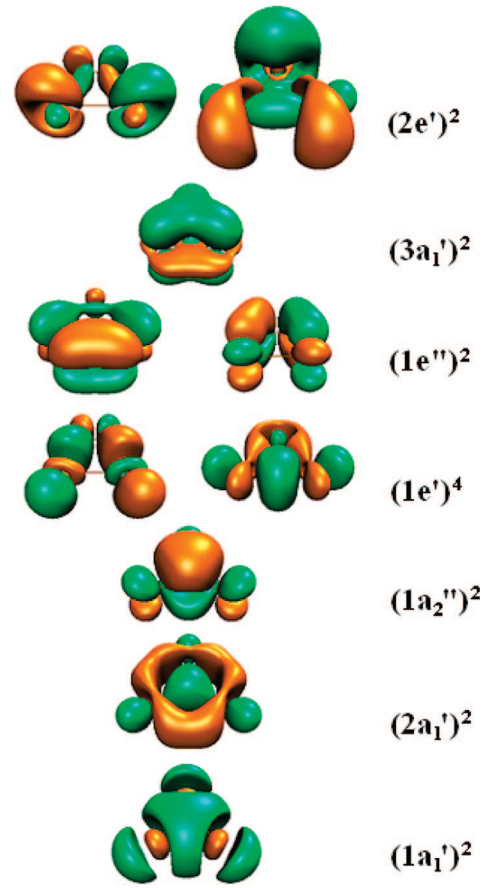

Figure 4. Pictures of the valence molecular orbitals for the Ta_3^- (D_{3h}, $^5A_1'$) ground state.

with band D (VDE ~ 2.2 eV). The sixth detachment channel is from $1a_2''(\beta)$, which should correspond to the intense band E. The computed VDE (2.61 eV) seems to be overestimated by about 0.22 eV, in comparison to the experiment (2.39 eV). The calculated VDEs for the next two detachment channels [$2a_1'(\beta)$ and $1e'(\alpha)$] are 2.74 and 2.87 eV, which agree well with the estimated VDEs for the two broad bands F (VDE ≈ 2.7 eV) and G (VDE ≈ 2.9 eV), respectively. There are several calculated one-electron detachment channels at higher binding energies. However, the PES spectra become very congested in the high binding energy side (Figure 1), suggesting that there are likely significant contributions from multielectron transitions due to strong electron correlation effects. Thus, quantitative assignments of this spectral region are no longer feasible on the basis of the one-electron calculations.

The assigned spectral features are given in Table 1, and the computed VDEs are plotted in Figure 1b as vertical bars. Overall, the pattern of the calculated VDEs for the low-lying transitions is in good agreement with the experimental PES spectra, lending considerable credence to the D_{3h} ($^5A_1'$) structure as the ground-state of Ta_3^-.

5.2. Chemical Bonding in Ta_3^- (D_{3h}, $^5A_1'$): All-Metal δ-Aromaticity. To further understand the structure and chemical bonding in Ta_3^-, we carried out a detailed MO analysis for the D_{3h} ($^5A_1'$) ground-state of Ta_3^-, as depicted in Figure 4. The fully occupied $1a_1'$ and 1e′ MOs form a σ bonding/antibonding pair and do not contribute to the net chemical bonding in Ta_3^-. The $2a_1'$ and 2e′ MOs form another σ bonding/antibonding pair, but the antibonding 2e′ orbital is half-filled, resulting in partial σ bonding contribution to

Ta_3^-. Analogously, the $1a_2''$ and $1e''$ MOs form a π bonding/antibonding pair and the half-filled $1e''$ orbital results in partial π bonding in Ta_3^-. The $3a_1'$ MO is a completely delocalized δ orbital, giving rise to δ aromaticity in Ta_3^-. The delocalized partial σ and π bonding in Ta_3^- makes it partially σ- and π-aromatic. Thus, Ta_3^- can be considered to possess multiple (partial σ-, partial π-, and δ-) aromatic characters. Interestingly, Ta_3^- is similar to the D_{3h} Hf_3 cluster, which has been recently reported as a triply (σ-, π-, and δ-) aromatic cluster because the antibonding $1e''$ and $2e'$ orbitals are unoccupied.

6. Conclusions

In conclusion, photoelectron spectroscopy is combined with density functional theory calculations to investigate the electronic structure and chemical bonding in the tantalum trimer cluster. PES spectra are obtained for Ta_3^- at several photon energies, revealing well-resolved low-lying electronic transitions and congested spectral feature in the high binding energy regime. The electron affinity of Ta_3 was determined to be 1.35 ± 0.03 eV. DFT calculations are performed at the B3LYP/Stuttgart+2f1g level to locate the ground-state and low-lying isomers for Ta_3 and Ta_3^-, yielding a quintet D_{3h} ($^5A_1'$) ground-state for the Ta_3^- anion and two nearly isoenergetic states C_{2v} ($^4A_1$) and D_{3h} ($^6A_1'$) as the lowest energy states for the Ta_3 neutral. The calculated detachment transitions from the D_{3h} ($^5A_1'$) anion ground-state is in good agreement with the experimental data. A detailed molecular orbital analysis shows that Ta_3^- is an interesting chemical species with multiple (δ-, partial π-, and partial σ-) d-orbital aromaticity, responsible for its highly symmetric D_{3h} structure.

Acknowledgment. The experimental work was supported by the U.S. National Science Foundation (Grant CHE-0749496) and performed at the W. R. Wiley Environmental Molecular Sciences Laboratory, a national scientific user facility sponsored by the U.S. DOE's Office of Biological and Environmental Research and located at the Pacific Northwest National Laboratory, operated for DOE by Battelle. X.H. gratefully acknowledges supports from the Natural Science Foundation of China (Grants 20641004 and 20771026) and the Natural Science Foundation of Fujian Province of China (No. 2008J0151).

Supporting Information Available: Relative energies in eV for selected low-lying isomers of Ta_3^- with different density functional methods. This material is available free of charge via the Internet at http://pubs.acs.org.

References and Notes

(1) Cotton, F. A.; Curtis, N. F.; Harris, C. B.; Johnson, B. F. G.; Lippard, S. J.; Mague, J. T.; Robinson, W. R.; Wood, J. S. *Science* **1964**, *145*, 1305.

(2) Wang, X. B.; Wang, L. S. *J. Am. Chem. Soc.* **2000**, *122*, 2096.

(3) Cotton, F. A.; Murillo, C. A.; Walton, R. A. *Multiple Bonds Between Metal Atoms*, 3rd ed.; Springer: New York, 2005.

(4) Nguyen, T.; Sutton, A. D.; Brynda, M.; Fettinger, J. C.; Long, G. J.; Power, P. P. *Science* **2005**, *310*, 844.

(5) Gagliardi, L.; Roos, B. O. *Nature* **2005**, *433*, 848.

(6) Roos, B. O.; Borin, A. C.; Gagliardi, L. *Angew. Chem., Int. Ed.* **2007**, *46*, 1469.

(7) (a) Frenking, G. *Science* **2005**, *310*, 796. (b) Radius, U.; Breher, F. *Angew. Chem., Int. Ed.* **2006**, *45*, 3006. (c) Frenking, G.; Tonner, R. *Nature* **2007**, *446*, 276. (d) Weinhold, F.; Landis, C. R. *Science* **2007**, *316*, 61.

(8) (a) Brynda, M.; Gagliardi, L.; Widmark, P. O.; Power, P. P.; Roos, B. O. *Angew. Chem., Int. Ed.* **2006**, *45*, 3804. (b) La Macchia, G.; Brynda, M.; Gagliardi, L. *Angew. Chem., Int. Ed.* **2006**, *45*, 6210. (c) Roos, B. O.; Malmqvist, P.; Gagliardi, L. *J. Am. Chem. Soc.* **2006**, *128*, 17000. (d) Kreisel, K. A.; Yap, G. P. A.; Dmitrenko, O.; Landis, C. R.; Theopold, K. H. *J. Am. Chem. Soc.* **2007**, *129*, 14162. (e) Merino, G.; Donald, K. J.; D'Acchioli, J. S.; Hoffmann, R. *J. Am. Chem. Soc.* **2007**, *129*, 15295. (f) La Macchia, G.; Gagliardi, L.; Power, P. P.; Brynda, M. *J. Am. Chem. Soc.* **2008**, *130*, 5104.

(9) For a recent perspective article on aromaticity in transition metal systems, see: Zubarev, D. Yu.; Averkiev, B. B.; Zhai, H. J.; Wang, L. S.; Boldyrev, A. I. *Phys. Chem. Chem. Phys.* **2008**, *10*, 257.

(10) (a) King, R. B. *Inorg. Chem.* **1991**, *30*, 4437. (b) Li, J. *J. Cluster Sci.* **2002**, *13*, 137. (c) Tsipis, A. C.; Tsipis, C. A. *J. Am. Chem. Soc.* **2003**, *125*, 1136. (d) Datta, A.; John, N. S.; Kulkarni, G. U.; Pati, S. K. *J. Phys. Chem. A* **2005**, *109*, 11647. (e) Wannere, C. S.; Corminboeuf, C.; Wang, Z. X.; Wodrich, M. D.; King, R. B.; Schleyer, P. v. R. *J. Am. Chem. Soc.* **2005**, *127*, 5701. (f) Chi, X. X.; Liu, Y. *Int. J. Quantum Chem.* **2007**, *107*, 1886.

(11) (a) Kuznetsov, A. E.; Corbett, J. D.; Wang, L. S.; Boldyrev, A. I. *Angew. Chem., Int. Ed.* **2001**, *40*, 3369. (b) Alexandrova, A. N.; Boldyrev, A. I.; Zhai, H. J.; Wang, L. S. *J. Phys. Chem. A* **2005**, *109*, 562. (c) Lin, Y. C.; Sundholm, D.; Juselius, J.; Cui, L. F.; Li, X.; Zhai, H. J.; Wang, L. S. *J. Phys. Chem. A* **2006**, *110*, 4244.

(12) Huang, X.; Zhai, H. J.; Kiran, B.; Wang, L. S. *Angew. Chem., Int. Ed.* **2005**, *44*, 7251.

(13) Zhai, H. J.; Averkiev, B. B.; Zubarev, D. Yu.; Wang; L. S.; Boldyrev, A. I. *Angew. Chem., Int. Ed.* **2007**, *46*, 4277.

(14) Li, S. D.; Miao, C. Q.; Guo, J. C. *Eur. J. Inorg. Chem.* **2008**, *8*, 1205.

(15) Averkiev, B. B.; Boldyrev, A. I. *J. Phys. Chem. A* **2007**, *111*, 12864.

(16) (a) Li, X.; Kuznetsov, A. E.; Zhang, H. F.; Boldyrev, A. I.; Wang, L. S. *Science* **2001**, *291*, 859. (b) Kuznetsov, A. E.; Birch, K. A.; Boldyrev, A. I.; Li, X.; Zhai, H. J.; Wang, L. S. *Science* **2003**, *300*, 622.

(17) Boldyrev, A. I.; Wang, L. S. *Chem. Rev.* **2005**, *105*, 3716.

(18) (a) Zhai, H. J.; Alexandrova, A. N.; Birch, K. A.; Boldyrev, A. I.; Wang, L. S. *Angew. Chem., Int. Ed.* **2003**, *42*, 6004. (b) Zhai, H. J.; Kiran, B.; Li, J.; Wang, L. S. *Nat. Mater.* **2003**, *2*, 827. (c) Zhai, H. J.; Wang, L. S.; Zubarev, D. Yu.; Boldyrev, A. I. *J. Phys. Chem. A* **2006**, *110*, 1689. (d) Sergeeva, A. P.; Zubarev, D. Yu.; Zhai, H. J.; Boldyrev, A. I.; Wang, L. S. *J. Am. Chem. Soc.* **2008**, *130*, 7244.

(19) Alexandrova, A. N.; Boldyrev, A. I.; Zhai, H. J.; Wang, L. S. *Coord. Chem. Rev.* **2006**, *250*, 2811.

(20) Collings, B. A.; Rayner, D. M.; Hackett, P. A. *Int. J. Mass Spectrom. Ion Processes* **1993**, *125*, 207.

(21) Fang, L.; Shen, X.; Chen, X.; Lombardi, J. R. *Chem. Phys. Lett.* **2000**, *332*, 299.

(22) Heaven, M. W.; Stewart, G. M.; Buntine, M. A.; Metha, G. F. *J. Phys. Chem. A* **2000**, *104*, 3308.

(23) Dryza, V.; Addicoat, M. A.; Gascooke, J. R.; Buntine, M. A.; Metha, G. F. *J. Phys. Chem. A* **2005**, *109*, 11180.

(24) Fa, W.; Luo, C.; Dong, J. *J. Chem. Phys.* **2006**, *125*, 114305.

(25) Wu, Z. J.; Kawazoe, Y.; Meng, J. *J. Mol. Struct.: THEOCHEM* **2006**, *764*, 123.

(26) (a) Wang, L. S.; Cheng, H. S.; Fan, J. *J. Chem. Phys.* **1995**, *102*, 9480. (b) Wang, L. S.; Wu, H. In *Cluster Materials*; Duncan, M. A., Ed.; Advances in Metal and Semiconductor Clusters, Vol. 4; JAI Press: Greenwich, CT, 1998; pp 299−343.

(27) (a) Wang, L. S.; Li, X. In *Clusters and Nanostructure Interfaces*; Jena, P., Khanna, S. N., Rao, B. K., Eds.; World Scientific: NJ, 2000; pp 293−300. (b) Akola, J.; Manninen, M.; Hakkinen, H.; Landman, U.; Li, X.; Wang, L. S. *Phys. Rev. B* **1999**, *60*, R11297. (c) Wang, L. S.; Li, X.; Zhang, H. F. *Chem. Phys.* **2000**, *262*, 53. (d) Zhai, H. J.; Wang, L. S.; Alexandrova, A. N.; Boldyrev, A. I. *J. Chem. Phys.* **2002**, *117*, 7917.

(28) Becke, A. D. *J. Chem. Phys.* **1993**, *98*, 1372.

(29) Lee, C.; Yang, W.; Parr, R. G. *Phys. Rev. B* **1988**, *37*, 785.

(30) Stephens, P. J.; Devlin, F. J.; Chabalowski, C. F.; Frisch, M. J. *J. Phys. Chem.* **1994**, *98*, 11623.

(31) Andrae, D.; Haeussermann, U.; Dolg, M.; Stoll, H.; Preuss, H. *Theor. Chim. Acta* **1990**, *77*, 123.

(32) Küchle, W.; Dolg, M.; Stoll, H.; Preuss, H. *Pseudopotentials of the Stuttgart/Dresden Group 1998*, revision August 11, 1998. http://www.theochem.uni-stuttgart.de/pseudopotentiale.

(33) Martin, J. M. L.; Sundermann, A. *J. Chem. Phys.* **2001**, *114*, 3408.

(34) Tozer, D. J.; Handy, N. C. *J. Chem. Phys.* **1998**, *109*, 10180.

(35) Frisch, M. J.; Trucks, G. W.; Schlegel, H. B.; Scuseri a, G. E.; Robb, M. A.; Cheeseman, J. R.; Zakrzewski, V. G.; Montgomery, J. A., Jr.; Stratmann, R. E.; Burant, J. C.; Dapprich, S.; Millam, J. M.; Daniels, A. D.; Kudin, K. N.; Strain, M. C.; Farkas, O.; Tomasi, J.; Barone, V.; Cossi, M.; Cammi, R.; Mennucci, B.; Pomelli, C.; Adamo, C.; Clifford, S.; Ochterski, J.; Petersson, G. A.; Ayala, P. Y.; Cui, Q.; Morokuma, K.; Malick, D. K.; Rabuck, A. D.; Raghavachari, K.; Foresman, J. B.; Cioslowski, J.; Ortiz, J. V.; Stefanov, B. B.; Liu, G.; Liashenko, A.; Piskorz, P.; Komaromi, I.; Gomperts, R.; Martin, R. L.; Fox, D. J.; Keith, T.; Al-Laham, M. A.; Peng, C. Y.; Nanayakkara, A.; Gonzalez, C.;

Challacombe, M.; Gill, P. M. W.; Johnson, B.; Chen, W.; Wong, M. W.; Andres, J. L.; Gonzalez, C.; Head-Gordon, M.; Replogle, E. S.; Pople, J. A. *Gaussian 03*, revision D.01; Gaussian, Inc.: Pittsburgh, PA, 2005.

(36) VMD (Visual Molecular Dynamics) : Humphrey, W.; Dalke, A.; Schulten, K. *J. Mol. Graphics* **1996**, *14*, 33.

(37) Li, S.; Alemany, M. M. G.; Chelikowsky, J. R. *J. Chem. Phys.* **2004**, *121*, 5893.

(38) Kietzmann, H.; Morenzin, J.; Bechthold, P. S.; Ganteför, G.; Eberhardt, W.; Yang, D. S.; Hackett, P. A.; Fournier, R.; Pang, T.; Chen, C. *Phys. Rev. Lett.* **1996**, *77*, 4528.

(39) Ziegler, T. *Chem. Rev.* **1991**, *91*, 651.

(40) (a) Yang, X.; Waters, T.; Wang, X. B.; O'Hair, R. A. J.; Wedd, A. G.; Li, J.; Dixon, D. A.; Wang, L. S. *J. Phys. Chem. A* **2004**, *108*, 10089. (b) Zhai, H. J.; Huang, X.; Cui, L. F.; Li, X.; Li, J.; Wang, L. S. *J. Phys. Chem. A* **2005**, *109*, 6019. (c) Huang, X.; Zhai, H. J.; Li, J.; Wang, L. S. *J. Phys. Chem. A* **2006**, *110*, 85. (d) Zubarev, D. Y.; Boldyrev, A. I.; Li, J.; Zhai, H. J.; Wang, L. S. *J. Phys. Chem. A* **2007**, *111*, 1648. (e) Zhai, H. J.; Li, S. G.; Dixon, D. A.; Wang, L. S. *J. Am. Chem. Soc.* **2008**, *130*, 5167.

JP806166H